

## Fabrication of inverted opal ZnO photonic crystals by atomic layer deposition

M. Scharrer, X. Wu, A. Yamilov, H. Cao, and R. P. H. Chang<sup>a)</sup>

Materials Research Institute, Northwestern University, Evanston, Illinois 60208

(Received 18 January 2005; accepted 14 March 2005; published online 7 April 2005)

We have fabricated three-dimensional optically active ZnO photonic crystals by infiltrating polystyrene opal templates using a low-temperature atomic layer deposition process. The polystyrene is removed by firing the samples at elevated temperatures, and reactive ion etching is used to remove the top layer of ZnO and expose the (111) photonic crystal surface. The resulting structures have high filling fractions, possess photonic band gaps in the near-UV to visible spectrum, and exhibit efficient photoluminescence. © 2005 American Institute of Physics.

[DOI: 10.1063/1.1900957]

Since photonic crystals (PhCs) were first proposed in 1987 by Yablonovitch<sup>1</sup> and John<sup>2</sup> they have been studied with great interest as a means of localizing light and modifying the emission properties of embedded light sources.<sup>3–5</sup> To study this effect, it requires efficient emission in the medium and a photonic band gap (PBG) that overlaps the emission spectrum. Material infiltration of three-dimensional (3D) colloidal crystals has been shown to be a versatile method to fabricate so-called “inverted opal” structures which have the long-range order, high filling fraction, and refractive index contrast required to exhibit a photonic band gap. Infiltration has been achieved by various methods, including chemical bath deposition,<sup>6</sup> electrodeposition,<sup>7,8</sup> sol-gel methods,<sup>9</sup> and low-pressure chemical vapor deposition (CVD)<sup>10,11</sup> (see Lopez<sup>12</sup> for a recent review), but achieving both high filling fractions and good luminescence properties of the material has proven difficult. Several groups have therefore studied the emission properties of lasing dyes or quantum dots infiltrated into opal or inverted opal backbones.<sup>3,5,13,14</sup>

Recently, atomic layer deposition (ALD) has been proposed as a promising route to fabricate inverted opal structures.<sup>15,16</sup> ALD is a modified CVD growth method in which a binary synthesis reaction is split into two self-limiting surface reactions by separate sequential exposures of the substrate to the chemical precursors. The resulting surface control and monolayer-by-monolayer growth sequence result in the formation of uniform and defect free films that are conformal to the substrate shape. In addition, ALD is a versatile and robust synthesis method which allows growth of a variety of materials under a wide range of conditions. Inverted opals of WN have been grown with ALD,<sup>15</sup> and King *et al.* have fabricated ZnS photonic crystals with high filling fractions and good luminescence properties.<sup>16</sup>

In this letter, we report the fabrication of inverted opal ZnO photonic crystals exhibiting strong PBGs and good luminescence using a low-temperature ALD technique. ZnO is a highly interesting optoelectronic material due to its potential as a short-wavelength light source. Its wide electronic band gap ( $\sim 3.37$  eV at room temperature) and high exciton binding energy ( $\sim 60$  meV) make it an efficient emitter in the near-UV spectrum. Its refractive index ( $\sim 2.2$ ) is too low to

produce a full (i.e., omnidirectional) photonic band gap but sufficient for the formation of directional pseudogaps. Results by Sumida *et al.*<sup>8</sup> have shown that infiltrating opal structures using electrodeposition to form ZnO is possible, but no optical measurements were reported.

Prior studies of ALD infiltration of opals have used silica opal templates, but the HF etching required to remove the silica would destroy the ZnO structure as well. For this study, polystyrene (PS) colloidal crystal templates were prepared from monodispersed carboxylate-modified PS spheres provided by Seradyne Inc. For our experiments, we used spheres with diameters ranging from  $\sim 160$  to 370 nm and monodispersities of about 2%–3%. The carboxylic acid groups give the spheres a hydrophilic surface and provide sites of covalent coupling for the precursor molecules, facilitating the growth of a dense film during ALD. Experiments with plain PS spheres resulted in low filling-fraction structures.

The templates were prepared using a vertical deposition technique detailed elsewhere.<sup>17,18</sup> Glass substrates were placed in vials with deionized water containing between 0.1 and 0.3 vol % PS spheres in suspension, depending on sphere size and intended film thickness. The water was then slowly evaporated at 50 °C in a drying oven. This method yielded PS opal films with controllable thicknesses between 20 and 100 layers and large single crystalline domains, oriented with the (111) planes of the face-centered-cubic structure parallel to the substrate surface. The templates were about 10 by 30 mm large and had uniform color throughout. During drying the opal film shrinks and it breaks up into domains that are several tens to hundreds of micrometers large, however.

ZnO was formed by infiltrating diethyl zinc  $\text{Zn}(\text{CH}_2\text{CH}_3)_2$  (DEtZn) and water as precursors into the opal templates using a continuous flow ALD reactor described elsewhere.<sup>19</sup> To avoid deformation or melting of the PS structures, the growth temperature was kept at 85 °C, below the glass transition temperature of PS. The chamber pressure during growth was kept at 10 Torr and a relatively slow flow of  $\text{N}_2$  carrier gas was maintained through the chamber. The precursors were heated to 40 °C to ensure high enough partial pressures for consistent dosing. One ALD reaction cycle consisted of a 2.0 s exposure to DEtZn, followed by a 30 s  $\text{N}_2$  purge, a 4.0 s exposure to  $\text{H}_2\text{O}$ , and another  $\text{N}_2$  purge. These high exposures resulted in relatively fast depletion of

<sup>a)</sup>Electronic mail: r-chang@northwestern.edu

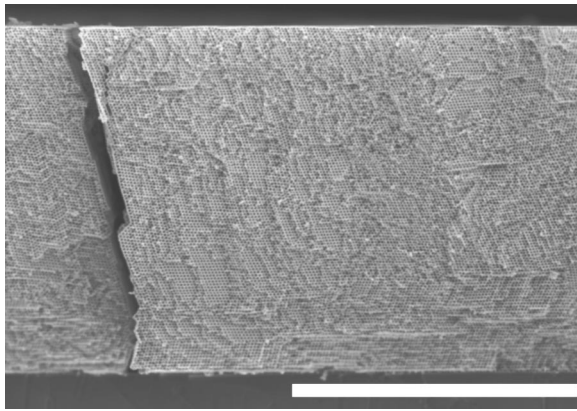


FIG. 1. SEM of a cleaved cross section of a 255 nm ZnO inverted opal structure (scale bar equals 20  $\mu\text{m}$ ).

the precursor reservoirs but were necessary to allow the precursor molecules to diffuse into and fully infiltrate the porous network of the opal structures. Shorter exposures resulted in incomplete infiltration unless the template thickness (i.e., the number of layers of PS spheres) was reduced accordingly. Each exposure sequence resulted in the growth of a partial monolayer of ZnO, with a corresponding growth rate of  $\sim 0.2$  nm per cycle on a flat substrate. The PS opal templates were infiltrated using 300 cycles for sphere sizes of 200 nm and below and 350 cycles for larger spheres. Once the open porosity is closed off an excess layer of ZnO formed on the outer surfaces of the templates, indicating complete infiltration. The PS spheres were then removed by firing the structures in air at 550  $^{\circ}\text{C}$  for 30 min, leaving an ordered fcc array of air holes in the ZnO matrix. The top layer of ZnO was etched away by reactive ion etching to expose the (111) crystal surface. RIE was done in a  $\text{CH}_4/\text{H}_2$  plasma at 300 W rf power and a pressure of 40 mTorr, followed by a cleaning step in oxygen plasma.

Figure 1 shows a cross section of an inverted opal structure. Even though this sample is relatively thick ( $>100$  layers of PS spheres) the ALD fully infiltrates the structure. The crack is caused by shrinkage of the template during drying and acts as an additional diffusion path for the precursor molecules. Firing of the structure causes some sintering and

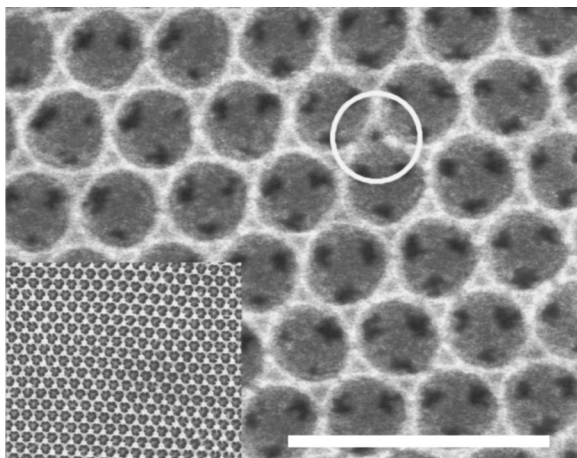


FIG. 2. SEM image of exposed (111) top surface of 356 nm ZnO inverted opals (scale bar equals 1  $\mu\text{m}$ ). The interstitial pores inherent in the infiltration process remain open after firing of the structure (circle). Inset: Lower magnification image of (111) surface.

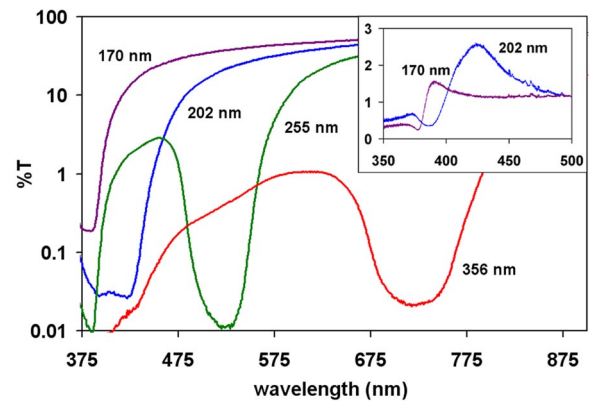


FIG. 3. (Color online). Transmission spectra of ZnO inverted opals measured in the (111) direction. As the band gap shifts towards the absorption edge with decreasing sphere size, the band-gap position becomes obscured. (The relatively low transmission of the 356 nm sample outside the band gap is due to its larger thickness.) Inset: Reflection peaks of the 170 and 202 nm structures at normal light incidence clearly show the existence of stop bands in the (111) direction near the absorption edge.

grain growth of the ZnO, as seen in Fig. 2, but did not change the lattice constant significantly ( $<2\%$  shrinkage from SEM analysis). The interstitial tetrahedral pores that are left between four adjacent spheres when the diffusion channels close off can still be seen. It should be noted that this porosity is predicted to increase the width of the band gap compared to an inverted opal structures without interstitial porosity.<sup>20</sup>

The ZnO films have uniform color after firing, and optical transmission measurements taken at zero incident angle clearly show the existence of partial PBGs in the (111) direction [Fig. 3]. By varying the sphere size we can shift the band gap position to any wavelength in the visible light spectrum. For small spheres ( $\leq 200$  nm) the short-wavelength band edge approaches the absorption edge of ZnO (at  $\sim 390$  nm) and the exact position of the PBG becomes difficult to determine by transmission. However, reflection spectra taken under normal incidence clearly reveal the existence of stop bands even very close to the absorption edge (inset of Fig. 3). The transmission and reflection spectra agree well with the results of variable-index band structure calculations (using a modified version of previously published software).<sup>21</sup> A comparison between the calculated and measured spectra indicates that our samples have high filling fractions and a ZnO refractive index close to the bulk value.

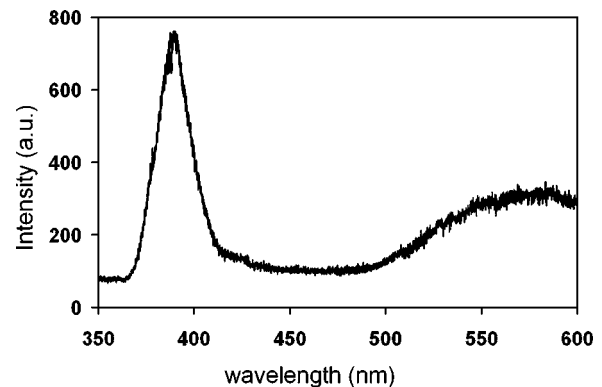


FIG. 4. PL spectrum of 202 nm ZnO inverted opal. This sample has no band gaps overlapping the emission spectrum.

This is consistent with previous results of inverted opal fabrication by ALD.

Photoluminescence measurements show efficient emission of the ZnO inverted opals in the UV as well as a defect emission band at longer wavelength. This proves that the ALD fabrication technique produces high quality films even at relatively low synthesis temperatures (Fig. 4).

For samples with band gaps overlapping the emission spectrum, we observed modification and suppression of emission due to the modified densities of photonic states, and a detailed investigation of the band structures and their influence on the PL and lasing properties of ZnO is currently being conducted.

In summary, we have used a low temperature ALD process to fabricate three-dimensional, optically active ZnO photonic crystals by infiltrating carboxylate-modified PS templates. ALD is capable of producing high filling fraction inverted opals of material with very good crystalline quality. The resulting ZnO structures exhibit clear photonic band gaps and strong photoluminescence, which makes them interesting candidates for studying the characteristics of modified spontaneous and stimulated emission in active photonic crystals.

This research project is supported by NSF Grant Nos. ECS-024457 and DMR-0353831.

<sup>1</sup>E. Yablonovitch, Phys. Rev. Lett. **58**, 2059 (1987).

<sup>2</sup>S. John, Phys. Rev. Lett. **58**, 2486 (1987).

<sup>3</sup>M. N. Shkunov, Z. V. Vardeny, M. C. DeLong, R. C. Polson, A. A.

Zakhidov, and R. H. Baughman, Adv. Funct. Mater. **12**, 21 (2002).

<sup>4</sup>S. G. Romanov, D. N. Chigrin, V. G. Solov'yev, T. Maka, N. Gaponik, A. Eychmuller, A. L. Rogach, and C. M. S. Torres, Phys. Status Solidi A **197**, 662 (2003).

<sup>5</sup>P. Lodahl, A. F. van Driel, I. S. Nikolaev, A. Irman, K. Overgaag, D. L. Vanmaekelbergh, and W. L. Vos, Nature (London) **430**, 654 (2004).

<sup>6</sup>J. E. G. J. Wijnhoven, L. Bechger, and W. L. Vos, Chem. Mater. **13**, 4486 (2001).

<sup>7</sup>P. Braun and P. Wiltzius, Adv. Mater. (Weinheim, Ger.) **13**, 482 (2001).

<sup>8</sup>T. Sumida, Y. Wada, T. Kitamura, and S. Yanagida, Chem. Lett. **30**, 38 (2001).

<sup>9</sup>S. L. Kuai, X. F. Hu, and V. V. Truong, J. Cryst. Growth **259**, 404 (2003).

<sup>10</sup>F. Meseguer, A. Blanco, H. Miguez, F. Garcia-Santamaria, M. Ibisate, and C. Lopez, Colloids Surf., A **202**, 281 (2002).

<sup>11</sup>V. G. Golubev, J. L. Hutchison, V. A. Kosobukin, D. A. Kurdyukov, A. V. Medvedev, A. B. Pevtsov, J. Sloan, and L. M. Sorokin, J. Non-Cryst. Solids **299**, 1062 (2002).

<sup>12</sup>C. Lopez, Adv. Mater. (Weinheim, Ger.) **15**, 1679 (2003).

<sup>13</sup>S. G. Romanov, D. N. Chigrin, C. M. S. Torres, N. Gaponik, A. Eychmuller, and A. L. Rogach, Phys. Rev. E **69**, 046606 (2004).

<sup>14</sup>A. F. Koenderink, L. Bechger, A. Lagendijk, and W. L. Vos, Phys. Status Solidi A **197**, 648 (2003).

<sup>15</sup>A. Rügge, J. S. Becker, R. G. Gordon, and S. H. Tolbert, Nano Lett. **3**, 1293 (2003).

<sup>16</sup>J. S. King, C. W. Neff, C. J. Summers, W. Park, S. Blomquist, E. Forsythe, and D. Morton, Appl. Phys. Lett. **83**, 2566 (2003).

<sup>17</sup>P. Jiang, J. F. Bertone, K. S. Hwang, and V. L. Colvin, Chem. Mater. **11**, 2132 (1999).

<sup>18</sup>S. L. Kuai, X. F. Hu, A. Hache, and V. V. Truong, J. Cryst. Growth **267**, 317 (2004).

<sup>19</sup>A. W. Ott and R. P. H. Chang, Mater. Chem. Phys. **58**, 132 (1999).

<sup>20</sup>K. Busch and S. John, Phys. Rev. E **58**, 3896 (1998).

<sup>21</sup>N. Stefanou, V. Yannopoulos, and A. Modinos, Comput. Phys. Commun. **132**, 189 (2000).